Supplemental Material for "Transport, multifractality, and the breakdown of single-parameter scaling at the localization transition in quasiperiodic systems"

Jagannath Sutradhar, Subroto Mukerjee, Rahul Pandit, and Sumilan Banerjee
Centre for Condensed Matter Theory, Department of Physics,
Indian Institute of Science, Bangalore 560012, India

S1. THOULESS CONDUCTANCE

The Thouless conductance, discussed in Sec.IIA of the main text, is defined as

$$g_T(E) = \frac{\delta E}{\Delta_E}, \tag{S1}$$

where Δ_E is the mean-level-spacing or the typical-level-spacing (i.e., geometric mean of the level spacings) and δE is the geometric mean of energy level shifts, $|\epsilon_A - \epsilon_P|$, over an energy window $[E-w, E+w]$, with width $w \gg \Delta_E$. Here ϵ_P and ϵ_A are eigenvalues of the Hamiltonian with periodic and anti-periodic boundary conditions, respectively. We calculate the energy spectrum by numerical diagonalization of the quasiperiodic Hamiltonians considered in the main text. The energy spectrum of the Aubry-Andre model has a Cantor-set structure with bands of states separated by a dense set of gaps [1–3]. We choose w to be much smaller than the width of the principal bands. Alternatively, $g_{\rm T}$ can be defined in terms of the mean energy level curvature under a twisted boundary condition or an Aharonov-Bohm flux in a ring geometry [4, 5]. We have checked that $g_{\rm T}$, obtained from mean-energy-level curvature, gives results similar to those from Eq. (S1). Because the latter does not require the computation of eigenvectors, we have used Eq. (S1) to calculate $g_{\rm T}$, reported in the main text. We obtain the mean, $\langle g_{\rm T}\rangle$, and the typical, $\langle \exp(g_{\rm T})\rangle$, conductances by averaging over ϕ. We also calculate $g_{\rm T}^{\infty}$, averaged over the whole energy spectrum, as shown in Fig. S1(a) for the critical point ($V = 1$) in $1d$. This shows the sharp resonances and various sequences of lengths with different power laws, as in Fig. 1(b) (main text) for $g_{\rm T}(E = 0)$.

We have also calculated $g_{\rm T}(L)$ in $1d$ for the irrational number $b = 1/\sigma_s = \sqrt{2} - 1$, the reciprocal of the silver ratio. As shown in Fig. S1(b), here also we get similar peaks in the conductance at system sizes related to the Pell numbers, i.e., $P_{n+1} = 2P_n + P_{n-1}$, with $P_0 = 1$ and $P_1 = 2$, such that $\sigma_s = \lim_{n\to\infty}(P_{n+1}/P_n)$.

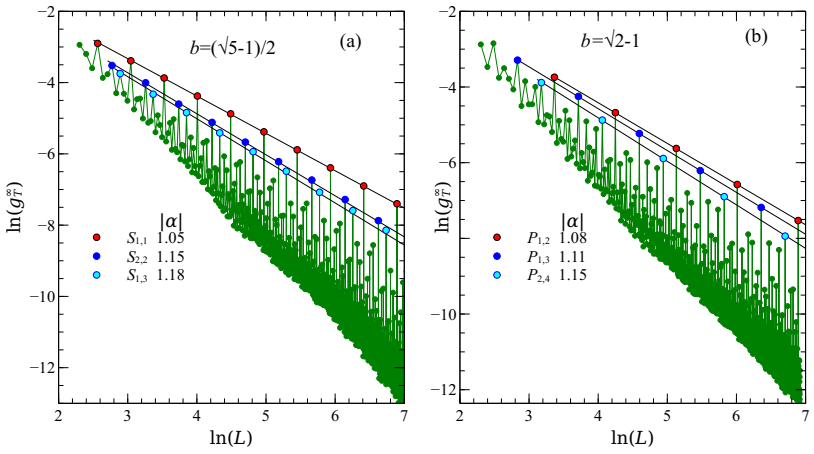

FIG. S1. (a) log-log plots of the infinite temperature (i.e. averaged over the full energy spectrum) Thouless conductance (g_T^{∞}) for $1d$, with the inverse of golden ratio as the irrational number (i.e., $b = (\sqrt{5}-1)/2$) in the potential, versus the system size L. $\mathcal{S}$'s are the same sequences described in Fig. 1. The conductances for different sequences of system sizes yield different exponents α, where $g_{\rm T} \propto L^{\alpha}$. (b) The analog of (a) with $b = (\sqrt{2}-1)$. P_{L_1,L_2} represents the sequence of system sizes (related to Pell numbers) started with seeds L_1 and L_2 (see S1). Both in (a) and (b), the peak of the conductance appears when the system size belongs to the respective sequences.

S2. MULTIFRACTAL ANALYSIS

Motivated by the strong-non monotonicity of $g_{\rm T}(L)$ in $1d$ [Figs. 1(a) and 1(b), main text] and multiple power laws in Fig. 1(b), we carry out a multifractal fluctuation analysis [6, 7] of the $g_{\rm T}(L)$ data, by analogy with the analysis of multifractal *time series*, i.e., $g_{\rm T}(i) \equiv g_{\rm T}(L_i)$ with $i = 1, \ldots, N$, where L_1 and L_N are the minimum and maximum system sizes studied, respectively. First, we do a cumulative sum of the data, i.e., $y(j) = \sum_{i=1}^{j} g_{\rm T}(i)$ for $j = 1, \ldots, N$. Then, to remove any trend from the data, we subtract moving average from each data point. The moving average $\bar{y}(j)$ is the average of $y(j)$'s over an interval (here we used $[j-13, j+13]$) around j. This gives us the residual sequence $\tilde{y}(j) = y(j) - \bar{y}(j)$. Now the residual sequence is divide into non-overlapping segments $j_s = 1, \ldots, N_s$ of width s, where N_s is the largest integer not larger than $N/s - 1$. The root mean square (rms) fluctuation is calculated for each segment, i.e.,

$$F_s(j_s) = \sqrt{\frac{1}{s} \sum_{j \in j_s} \bar{y}^2(j)} \quad ; \tag{S2a}$$

and we obtain the oder-q moments

$$P_q = \left(\frac{1}{N_s} \sum_{j_s=1}^{N_s} F_s^q(j_s) \right)^{1/q} \quad . \tag{S2b}$$

These moments follow multifractal power-law scalings with the segments length s, i.e., $P_q(s) \sim s^{h(q)}$, as shown for $q = 3$ and 4 in Fig. 1(e) (main text) at the $1d$ critical point.

To quantify the multifractality, we can obtain the singularity spectrum through a Legendre transform, $f(\alpha) = q[\alpha - h(q)] + 1$, with $\alpha = \partial[qh(q) - 1]/\partial q$. For a more refined multifractal analysis, we use a wavelet transform of the Thouless conductance data, namely, we convolve the data set with a fixed-order derivative of the Gaussian funtion, $G^n(x) = d^n(e^{-x^2/2})/dx^n$. This removes any polynomial trend in the data upto order $n-1$, leaving only the singular dependence. Now this power can be extracted via a log-log fit and, thus, the singularity spectrum can be obtained. To this end, we use the codes of ref.[8]. In our calculation we use the fourth order derivative of Gaussian function. The resulting singularity spectra $f(\alpha)$ for the $1d$ Thouless conductances in the metallic phase and at the critical point are shown in Fig. 1(f). The singularity spectra computed by using the moments in Eqs.S2 are qualitatively similar to those obtained via the wavelet-transform method.

1. *Wavefunction Multifractality*

The conductance multifractality obtained in the preceding section from the L dependence of Thouless conductance directly characterizes the violation of the assumption of monotonicity in the single-parameter-scaling theory. As discussed in the main text, this kind of multifractality in quasiperiodic system is quite different from well-known the wavefunction multifractality at the critical point between a metal and an insulator in a random system, e.g., at the 3d Anderson transition [9]. Conventionally, the multifractality of critical single-particle eigenstates ψ_r is analyzed in terms of the moments of the wavefunction amplitude [9], i.e., $P_q^{\psi} = \sum_r |\psi_r|^{2q}$, which, upon disorder averaging, follow a power-law scaling $\langle P_q \rangle \sim L^{-\tau(q)}$, with an exponent $\tau(q) = d(q-1) + \Delta_q$ that depends non-trivially on q, as characterized by the anomalous dimension $\Delta(q)$. We show in Fig. S2 that, much like at the $3d$ Anderson criticality [9], the critiacal wavefunctions of quasiperiodic system also possess the usual multifractality in $1d$, as characterized by the singularity spectrum obtained from the Legendre transform of $\tau(q)$ [10].

S3. LANDAUER CONDUCTANCE IN $1d$

The Schrödinger equation for the $1d$ Hamiltonian, given in Eq. (1), can be written in the latttice basis, $\{\psi_r\}$ in the following way:

$$\begin{pmatrix} \psi_{r+1} \\ \psi_r \end{pmatrix} = \begin{pmatrix} \epsilon_r & -1 \\ 1 & 0 \end{pmatrix} \begin{pmatrix} \psi_r \\ \psi_{r-1} \end{pmatrix} = M_r \begin{pmatrix} \psi_r \\ \psi_{r-1} \end{pmatrix} = \prod_{i=1}^{r} M_i \begin{pmatrix} \psi_1 \\ \psi_0 \end{pmatrix} = \mathbf{M} \begin{pmatrix} \psi_1 \\ \psi_0 \end{pmatrix} \quad ; \tag{S3}$$

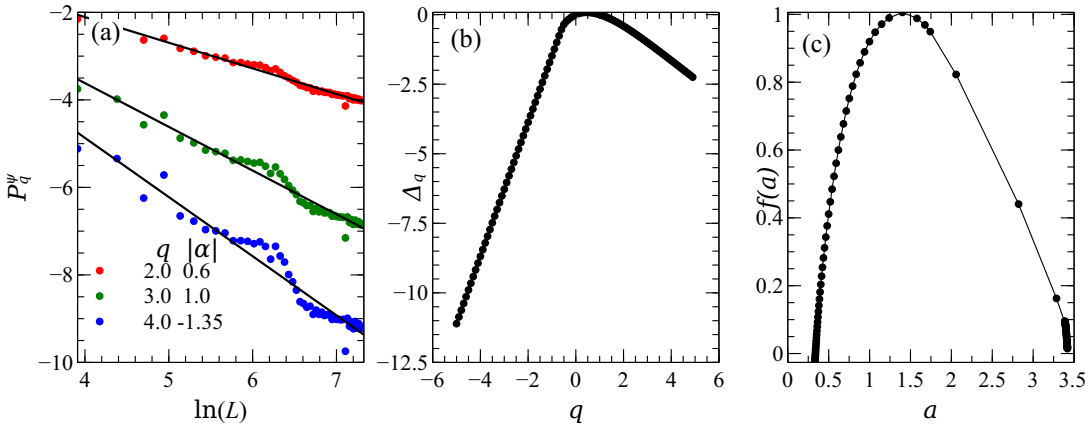

FIG. S2. (a) The scaling of different moments of the wave function of the 1D Hamiltonian, $P_q^\psi \sim L^{-\alpha}$, averaged over all energy, is shown here. (b) Shows the anomalous dimension Δ_q. (c) The singularity spectrum $f(\alpha)$ shows the multifractal nature of the wave function.

here, $\epsilon_r = E - 2V\cos(2\pi br + \phi)$ and E is the energy of interest. By iterating this equation, we can calculate the amplitude at the end points, given the two starting amplitudes. This transfer matrix $\mathbf{M}$ is related to the transmission matrix $\mathbf{T}$ via [11],

$$\mathbf{T} = \mathbf{Q}^{-1}\mathbf{M}\mathbf{Q}\ , \tag{S4}$$

where

$$\mathbf{Q} = \begin{pmatrix} 1 & 1 \\ e^{-ik} & e^{ik} \end{pmatrix}. \tag{S5}$$

Here the disordered region is considered to exist for $N > i > 0$ and $V = 0$ at all other points, with the transmitted wave amplitudes $\psi_{-1} = e^{ik}$ and $\psi_0 = 1$ for a wave propagating from the $i > N$ region to the region $i < 0$. The Landauer conductance is given by

$$g_{\rm L} = \frac{|t|^2}{|r|^2}, \tag{S6}$$

where t and r are, respectively, the transmission and reflection amplitudes in the transmission matrix. The Landauer conductance $g_{\rm L}(L)$ is shown in Figs. S3(a)-(d) for the metallic and critical states. The strong non-monotonicity in $g_{\rm L}(L)$ is evident.

S4. KUBO CONDUCTANCE

The open-system (dimensionless) conductance at the energy E for the system described by the quasiperiodic Hamiltonians [Eqs.(1) and (A1)], connected with non-interacting leads at the two ends along x direction, is given by the Kubo formula [12, 13],

$$g_{\rm K}(E) = 2{\rm Tr}[\hat{I}^x(x)\hat{G}''(E)\hat{I}^x(x')\hat{G}''(E)]\ , \tag{S7}$$

where G" $= (1/2i)(G^- - G^+)$ is obtained in terms of the Green functions $G^{\pm}(E) = (E - H \pm i\eta)^{-1}$, H being the Hamiltonian of the whole system including the leads. The current operator is

$$\hat{I}(j) = it\sum_l (|j-1,l\rangle\langle j,l| - |j,l\rangle\langle j-1,l|)\ , \tag{S8}$$

here l is the index that represents sites on any slice j perpendicular to the direction x. The conductance then simplifies to

$$g_{\rm K} = 2{\rm Tr}[2G''(j,j)G''(j-1,j-1) - G''(j-1,j)^2 - G''(j,j-1)^2]. \tag{S9}$$

The trace is over l, i.e, in the transverse direction. We evaluate the conductance by calculating the Green functions in Eq. (S9) via the standard recursive Green's function method described in Refs. [13–15]. The attached leads have the same width as that of the system; and we use hard-wall or open boundary condition in the transverse directions.

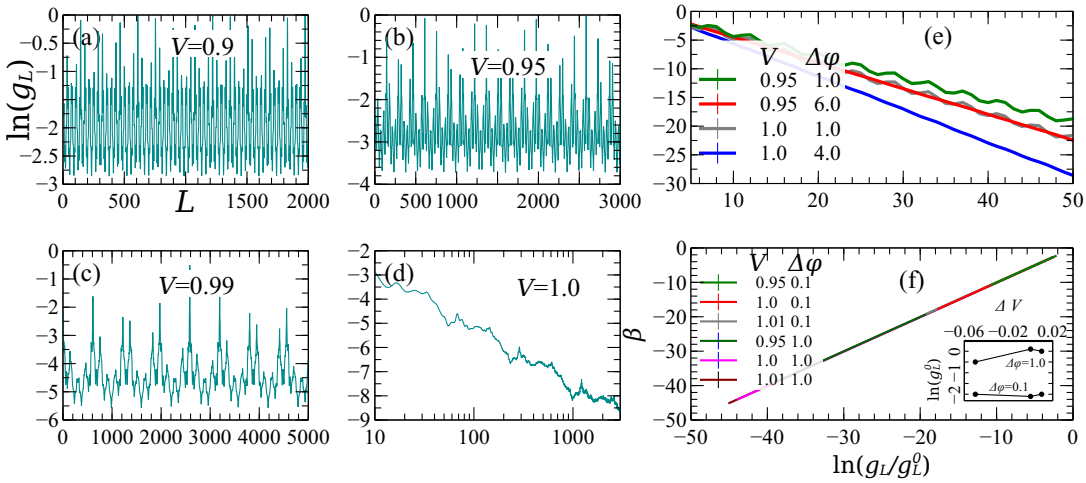

FIG. S3. (b)-(e) have the same axes labeling as (a). (a)-(d) $g_{\rm L}(L)$ for $1d$, both on the metallic side and at the critical point, are shown. (e) In the presence of randomly chosen phase at each site, from a uniform random disorder $[-\Delta\phi/2, \Delta\phi/2]$, the system becomes insulator for any nonzero value of V and $\Delta\phi$, which indicates the perturbation to be relevant. For a weak phase disorder the monotonicity of $g_{\rm L}(L)$ is still present. The data points are averaged over 3000 disorder realization. (f) Ignoring the L dependent fluctuation in weak disorder a continuous β function is obtained, hence the single-parameter scaling theory is recovered for the large length scale behavior of the conductance.

S5. BETA FUNCTION CALCULATIONS

To extract the β functions in Fig. 3 (main text), we carry out linear fitting for the $\ln g$ vs. $\ln L$ curves in the region $V \leq 1$; and, for $V > 1$, we do the same for $\ln g$ vs. L curves. This gives a power-law dependence of the conductance on L for metallic phase ($V \leq 1$) and an exponential dependence in the insulating regime ($V > 1$). The scaling-theory β function, $\beta(g) = d\ln g/d\ln L$, is calculated by taking the logarithmic derivative of the fitting curves. In $3d$, close to the critical point. we perform a scaling collapse of the data following Ref. [16]. To this end, we assume a single-parameter finite-size scaling form for the conductance, namely,

$$\ln g = \mathcal{F}(\Psi L^{1/\nu}) \ . \tag{S10}$$

The relevant scaling variable Ψ, in terms of the dimensionless parameter $v = (V - V_c)/V_c$, is approximated as $\Psi = \Psi_1 v + \Psi_2 v^2$; and we expand the scaling function $\mathcal{F}$ upto third-order in its argument. We minimize the quantity $\sum_i (\ln g_i - \mathcal{F}(\Psi_i L_i^{1/\nu}))^2$ to obtain the fitting parameters V_c, ν, Ψ_1, Ψ_2 and the coefficients of the third-order polynomial, where the index i represents each point of the data set $\{V, L\}$. Once the scaling function $\mathcal{F}(x)$ is known in terms of these parameters, we calculate the smooth β function in $3d$ near the metal-insulator transition at $V_c \simeq 2.2$, as shown in Fig. 3(d)

1. *Effects of phase disorder*

In Fig. S3(f), the results for $\beta(\tilde{g}_{\rm L})$ are shown, for a $1d$ model, where we modify the quasiperiodic potential in Eq. (1) from $\cos(2\pi br + \phi)$ to $\cos(2\pi br + \phi_r)$, with ϕ_r an uncorrelated random phase at each site, chosen uniformly from $[-\Delta\phi/2, \Delta\phi/2]$. The phase randomness, even if weak, leads to localization, as is evident from the exponential decay of the conductance with L in Fig. S3(e), even for $V < 1$. As expected for a random system, one gets back a continuous β function, by considering the conductance dependence on the long window of system sizes, i.e., by ignoring the non-monotonicity with L at small lengths, for weak strength of the randomness, in contrast to that in Fig. 3 (b). As shown in Fig. S3(e), the bare $g_{\rm L}(L)$ has a non-monotonic behavior with L in the presence of weak phase randomness, but the non monotonicity goes away as the randomness increases, completely restoring single-parameter-scaling theory, even for moderate strengths of disorder.

[1] Barry Simon, "Almost periodic Schrödinger operators: A Review," Advances in Applied Mathematics **3**, 463 – 490 (1982).

[2] S. Ostlund and R. Pandit, "Renormalization-group analysis of the discrete quasiperiodic Schrödinger equation," Phys. Rev. B **29**, 1394–1414 (1984).

[3] J. B.● Sokoloff, "Unusual band structure, wave functions and electrical conductance in crystals with incommensurate periodic potentials," Physics Reports **126**, 189 – 244 (1985).

[4] E. Akkermans, "Twisted boundary conditions and transport in disordered systems," Journal of Mathematical Physics **38**, 1781–1793 (1997).

[5] D. Braun, E. Hofstetter, A. MacKinnon, and G. Montambaux, "Level curvatures and conductances: A numerical study of the thouless relation," Phys. Rev. B **55**, 7557–7564 (1997).

[6] J. W. Kantelhardt, "Fractal and Multifractal Time Series," ArXiv e-prints (2008), arXiv:0804.0747 [physics.data-an].

[7] W. Zhou, Y. Dang, and Gu R., "Efficiency and multifractality analysis of CSI 300 based on multifractal detrending moving average algorithm," Physica A **392**, 1429–1438 (2013).

[8] A. L. Goldberger, L. A. N. Amaral, L. Glass, J. M. Hausdorff, P. Ch. Ivanov, R. G. Mark, J. E. Mietus, G. B. Moody, C.-K. Peng, and H. E. Stanley, "PhysioBank, PhysioToolkit, and PhysioNet: Components of a New Research Resource for Complex Physiologic Signals," Circulation **101**, e215– e220 (2000).

[9] F. Evers and A. D. Mirlin, "Anderson transitions," Rev. Mod. Phys. **80**, 1355–1417 (2008).

[10] D. Dominguez, C. Wiecko, and J. V. Jose, "Wavefunction and resistance scaling for quadratic irrationals in Harper's equation," Phys. Rev. B **45**, 13919 (1992).

[11] P. Markos, "Numerical Analysis of The Anderson Localization," Acta Physica Slovaca **56**, 561–686 (2006).

[12] D. S. Fisher and P. A. Lee, "Relation between conductivity and transmission matrix," Phys. Rev. B **23**, 6851–6854 (1981).

[13] P. A. Lee and D. S. Fisher, "Anderson localization in two dimensions," Phys. Rev. Lett. **47**, 882–885 (1981).

[14] A. MacKinnon and B. Kramer, "The scaling theory of electrons in disordered solids: Additional numerical results," Zeitschrift für Physik B Condensed Matter **53**, 1–13 (1983).

[15] J. A. Verges, "Computational implementation of the Kubo formula for the static conductance: application to two-dimensional quantum dots," Computer Physics Communications **118**, 71–80 (1999).

[16] K. Slevin, P. Markoš, and T. Ohtsuki, "Reconciling conductance fluctuations and the scaling theory of localization," Phys. Rev. Lett. **86**, 3594–3597 (2001).